

ANL/FPP/TM--212

ANL/FPP/TM-212

DE87 007530

ARGONNE NATIONAL LABORATORY
9700 South Cass Avenue
Argonne, Illinois 60439

SELF-PUMPING IMPURITY CONTROL SYSTEMS FOR INTOR

by

J. N. Brooks, R. F. Mattas, D. L. Smith, and A. M. Hassanein

Fusion Power Program

January 1987

Work supported by

Office of Fusion Energy
U.S. Department of Energy
Under Contract W-31-109-ENG-38

DISCLAIMER

This report was prepared as an account of work sponsored by an agency of the United States Government. Neither the United States Government nor any agency thereof, nor any of their employees, makes any warranty, express, or implied, or assumes any legal liability or responsibility for the accuracy, completeness, or usefulness of any information, apparatus, product, or process disclosed, or represents that its use would not infringe privately owned rights. Reference herein to any specific commercial product, process, or service by trade name, trademark, manufacturer, or otherwise does not necessarily constitute or imply its endorsement, recommendation, or favoring by the United States Government or any agency thereof. The views and opinions of authors expressed herein do not necessarily state or reflect those of the United States Government or any agency thereof.

RECEIVED
FEB 10 1987

TABLE OF CONTENTS

	Page
Abstract.....	1
Introduction.....	1
Self-Pumping Concept.....	2
Trapping Material Characteristics.....	3
System 1 - Slot Divertor.....	7
System 2 - Divertor Plate Trapping.....	14
Conclusion.....	18
References.....	20

LIST OF FIGURES

Figure No.	Caption	Page
1	Self-pumping slot divertor concept.....	9

LIST OF TABLES

Table No.	Caption	Page
1	Potential Benefits of Self-Pumping for INTOR.....	3
2	Entrapment Probability (%) as a Function of Incident Helium Ion Energy.....	6
3	Estimated Properties of Helium Trapping Materials.....	8
4	INTOR - Slot Self-Pumped Divertor.....	11
5	INTOR - Self-Pumped Divertor, System #2.....	15
6	Fraction of Injected Trapping Material Entering the Edge Plasma as a Function of Injection Location. From ZTRANS Monte Carlo Simulations for S_N Injection.....	18

SELF-PUMPING IMPURITY CONTROL SYSTEMS FOR INTOR
J. N. Brooks, R. F. Mattas, D. L. Smith, and A. M. Hassanein

ABSTRACT

Two self-pumping systems have been examined for use as the INTOR impurity control system. The systems work by trapping helium in freshly deposited metal surface layers on or near the divertor plate. A slot divertor concept using vanadium or other trapping material appears to be both feasible and mechanically simple, and offers significant advantages in cost, reduced complexity, and helium pumping efficiency for the INTOR design.

Introduction

Two self-pumping (helium burial) impurity control systems have been examined conceptually for INTOR: (1) plenum region trapping and (2) divertor plate trapping. Although there are uncertainties in materials properties and plasma transport issues, both systems appear to be feasible.

For a plenum type self-pumping system, reflected helium from the divertor region plasma is trapped on a surface not directly exposed to the plasma. Such a system reduces concerns about plasma contamination by the trapping material and temperature limits of the trapping material. The major issue for this design is helium trapping efficiency at low implantation energies. Helium is known to be trapped at 100-1000 eV impingement energies but there is sparse data for lower energies. Based on available information it appears that sufficient trapping will occur at energies as low as 30-50 eV. This would be adequate for an effective plenum self-pumping system. A plenum system based on a slot divertor concept is outlined. This appears to be a simple and robust design and is recommended as a reference self-pumped system.

For the divertor plate system, helium is trapped on the outer (large minor radius) portion of both the inner and outer collector plates. Trapping on the outer portion minimizes the plasma contamination produced by injection of trapping materials, and minimizes the heat load on the trapping sites. Vanadium is a leading candidate trapping material for this system. Transport code calculations were performed to assess the effect of trapping material injec-

tion on the plasma. These predict a very low concentration ($\sim 0.01\%$) of trapping material in the main plasma, resulting from the self-pumping system.

Benefits of the self-pumping system for INTOR appear to be significant. An order of magnitude reduction in the vacuum pumping system (ducts, pumps, and penetration shielding) could be realized. This could increase reliability, reduce cost, and free up space for nuclear and tritium breeding modules. A reduction in tritium recycling and refueling also results. In addition, self-pumping may offer higher helium removal efficiency.

Self-Pumping Concept

The self-pumping concept was proposed¹ as a means of simplifying impurity control in a fusion reactor. The basic concept is to remove helium in-situ by trapping in freshly deposited metal surface layers of a limiter or divertor. The trapping material is added to the surface at an average rate of 3-5 times the α -production rate to maintain an effective trapping surface. Trapping material can be added by injecting pellets or exposing rods, etc. to the edge or scrapeoff plasma where the material is ablated, vaporized and transported to the trapping surface. A key requirement is for the deposited material to trap helium much better than hydrogen. It has been demonstrated experimentally that nickel preferentially traps helium² and that several other materials (iron, vanadium, niobium, molybdenum, and tantalum) are believed to be capable of preferential trapping. The selective trapping in certain metals is a result of the negligible solubility of helium in the lattice. The injected helium will diffuse through the lattice until it reaches a nearby trapping site where it can be trapped. Hydrogen, on the other hand, remains in solid solution until it diffuses to the surface and escapes. Other plasma contaminants, notably oxygen, can be removed by the self-pumping system by chemically combining with the deposited metal.

Benefits of the self-pumping system, for a steady-state tokamak reactor, are the elimination of all vacuum ducts, pumps, and penetration shielding (except for a very small startup system), and the reduction of tritium recycle and refueling. For INTOR, in a pulsed mode of operation, there is a need to pump the plasma chamber between burns. A hydrogen pumping system is therefore required. However, this pumping system can be an order of magnitude smaller than a system needed for pumping during the burn. For example, for the refer-

ence INTOR divertor design there are 12 divertor modules each with a separate pumping duct. For a self-pumped system eleven ducts could be removed, leaving only one for between-burn pumping of the neutral gas.

Based on a plasma chamber volume of $\sim 300 \text{ m}^3$ and a single duct/pump speed of $\sim 25 \text{ m}^3/\text{s}$, adequate pumpdown could be achieved in under one minute. The single duct/pump could also be used during the burn if needed, e.g., for density control during neutral beam injection. Several ducts could also be retained, if required, for shorter dwell times, and still result in a large vacuum system reduction.

The potential benefits of self pumping for INTOR are outlined in Table 1. The cost savings due to self pumping have not been assessed for INTOR but savings of 35-90 M\$ have been estimated for various commercial fusion reactor designs.³ For INTOR, improvements in reliability and availability may be at more important than the cost savings.

TABLE 1. Potential Benefits of Self-Pumping for INTOR

-
- Elimination of $\sim 90\%$ of vacuum ducts, pumps, penetration shielding.
 - Reduction of $\sim 90\%$ in tritium pumping, processing, refueling.
 - Cost savings and increase in mass utilization factor.
 - Improved reliability/availability.
 - Vacuum duct space could be used for tritium breeding and/or other nuclear test modules.
 - Possibly much better ($\sim 10 \times$) helium removal efficiency than standard vacuum pumping.
-

Trapping Material Characteristics

A general discussion of trapping material properties is given in Ref. (1, 3). Important properties include the hydrogen and helium interactions with the material, thermal conductivity, and mechanical properties. For INTOR the material requirements are less stringent than for commercial reactors, because of the shorter operating time. For all applications the most important property is the helium trapping fraction. This determines the amount of material that must be added to the trapping surfaces. A related parameter is the sticking coefficient, i.e., the probability that a helium atom is trapped for a single impingement. These two parameters are closely related, however, the

helium trapping fraction will be greater or equal to the sticking coefficient because of multiple impingements.

Numerous experiments have shown that at relatively low doses ($\phi < 10^{22} \text{ m}^{-2}$) helium is effectively trapped in vacancies or small helium bubbles. At doses above a critical dose, ϕ_c , the implanted surface layer saturates and helium is re-emitted. In most of those experiments however the injected helium energies were in the KeV range. At low energies the surface plays an important role and its effects are evidenced by the measured gas loss. This is due to the failure of saturation fluences at energies below a few KeV to produce the drastic surface morphological modifications that characterize the higher energy bombardments. Only very few experiments have studied helium retention at very low energies (<100 eV).

In one experiment⁴ low energy helium ions were injected into 304 stainless steel, polycrystalline nickel foil and single crystal nickel targets and the gas evolution rate was monitored during post-bombardment annealing. Table 2 shows the measured entrapment probability for a stainless steel target for various incident helium ion energies up to 1 KeV. The entrapment coefficient reaches a maximum of about 0.7 at an incident ion energies of slightly above 1 KeV. At these energies the experimental results indicate that a significant fraction of the implanted gas persists in the target up to the melting point. That was confirmed by the copious release of gas observed when a target was actually melted.⁴ Stainless steel is a complex alloy where gas becomes trapped at impurities and precipitates from which it is released over a wide range of activation energies extending up to the melting point. Fewer types of defects will likely be present in pure metals.

Table 2 also shows the entrapment probability for different incident helium energies for both random nickel single crystal and polycrystalline nickel targets. The probability of trapping is almost a factor of 10 greater in the polycrystalline sample at energies equal or lower than 100 eV. Since at these energies the incident ions are not capable of producing displacement the higher entrapment probability may be due to the existence of other types of trapping sites inside the target such as grain boundaries.

In another study⁵ low energy helium ions were injected into Ni<100> single crystal substrates. Studies of the helium evolution spectra were obtained for different ion energies and fluences and nickel substrate temperature dur-

ing implantation. Table 2 compares the measured helium trapping coefficient for two different fluences at various incident ion energies. Again, the very low trapping coefficient for energies below 100 eV reflects the lack of available sites and the inability of the low energy helium to cause atomic displacement and create more trapping sites. This large increase in the trapping coefficient at higher fluences can be attributed to the growth, and eventual dominance of the agglomeration associated traps which contribute to gas release at higher temperatures in the so-called C-band peaks.⁶ A similar increase in helium trapping probability with increasing fluence has also been observed experimentally in randomly oriented single crystal nickel. The helium gas release is found in general to follow relatively well resolved peaks, some of which seem to depend strongly on both ion energy and fluence.⁵ The relative entrapment probability at higher implantation temperatures (normalized to implantation at 350°K) for each resolvable peak is given in Ref. 5. It is shown that at higher implantation temperatures the helium entrapment probability decreases sharply. For example, at an implantation temperature greater than 700°K for 1 KeV helium ion incident on nickel single crystal the entrapment probability decreased by about an order of magnitude or more compared to that of implantation at 350°K. This drastic reduction in the entrapment probability at higher implantation temperatures may be explained by a possible formation of different kind of defects such as singly occupied divacancies during implantation. The fact that these di-vacancies are expected to be mobile in the temperature range between 350 and 550°K offers one possible explanation for the reduced trapping due to gas migration to the surface.⁷

There are several major differences between most of the previous experiments and the actual conditions in a reactor system. One factor is the continuous and simultaneous deposition and build-up of the trapping material along with helium ions. This continuous deposition may help maintain a roughly uniform helium profile distribution in the material which may increase the retention. It also helps keeping the accumulated dose below ϕ_c the critical dose necessarily to cause blistering. However, depending on the characteristics and integrity of the redeposited trapping material the helium retention could even be lower than in the case without continuous deposition. This can happen, for example, if the redeposited material contains many interconnected porosity to the surface. Another important factor is the synergistic effect

TABLE 2. Entrapment Probability (Z) as a Function of Incident Helium Ion Energy

Helium Ion Energy (eV)	Stainless Steel* $\phi=1.4 \times 10^{14}$ ion cm ⁻²	Nickel*		Nickel** <100> single crystal	
		Random Single Crystal	Polycrystalline	$\phi=3 \times 10^{13}$ ion cm ⁻²	$\phi=3 \times 10^{14}$ ion cm ⁻²
30	--	<1	10	--	--
50	10	2	30	1	1
100	20	12	55	1.5	2
200	34	45	70	5	10
400	48	60	80	20	50
500	53	65	82	30	52
1000	67	70	85	50	60

Most of the numbers given are interpolations between measured values.

*See Reference 4.

**See Reference 5.

from simultaneous bombardment and implantation of protium, deuterium, and tritium in the redeposited material. This synergistic effect must be evaluated; it may result in reducing helium retention in the trapping material. This may be because both hydrogen (and its isotopes) and helium will compete roughly for the same amount of traps. However, because of the neutron radiation generated traps in a real fusion reactor environment the helium retention may increase substantially especially at low operating temperatures. It is important to note that several candidate trapping materials have been identified, therefore increasing the chance of selecting a suitable material.

Several important factors need to be studied experimentally in detail to firmly establish the parameters for helium retention and release since they are crucial to the successful operation of the self-pumped reactor concept. The simultaneous injection of the low energy helium ions and the structure and properties of the redeposited material are essential factors which need to be assessed before defining acceptable operating ranges for this concept. The role of higher implantation temperatures in determining the net trapping coefficient is very important since this could limit and constrain the operation of the reactor. The synergistic effect of simultaneous bombardment of the trapping material is also very important and needs to be studied to determine the overall retention coefficient. The neutron generated trapping sites in a fusion reactor environment are also likely to be very important. The neutron irradiation could substantially increase helium trapping.

Based on the above considerations, we are optimistic that impingement energies of 50-100 eV will permit adequate trapping fractions. Higher impingement energies would tend to result in even more effective trapping. Table 3 lists the estimated values of trapping and other parameters for the present analysis.

SYSTEM 1 - Slot Divertor

There are 3 key issues for a plenum type self-pumping system: (1) helium trapping at low energies, (2) means of introducing the trapping material, and (3) recycling of hydrogen. A trapping site far from the plasma would present difficulties in all three areas. We conclude that a preferable and probably necessary system is one that is as near to the plasma as possible. A plenum

based system, called a slot divertor, has been developed conceptually to examine the feasibility issues of plenum self-pumping.

TABLE 3. Estimated Properties of Helium Trapping Materials

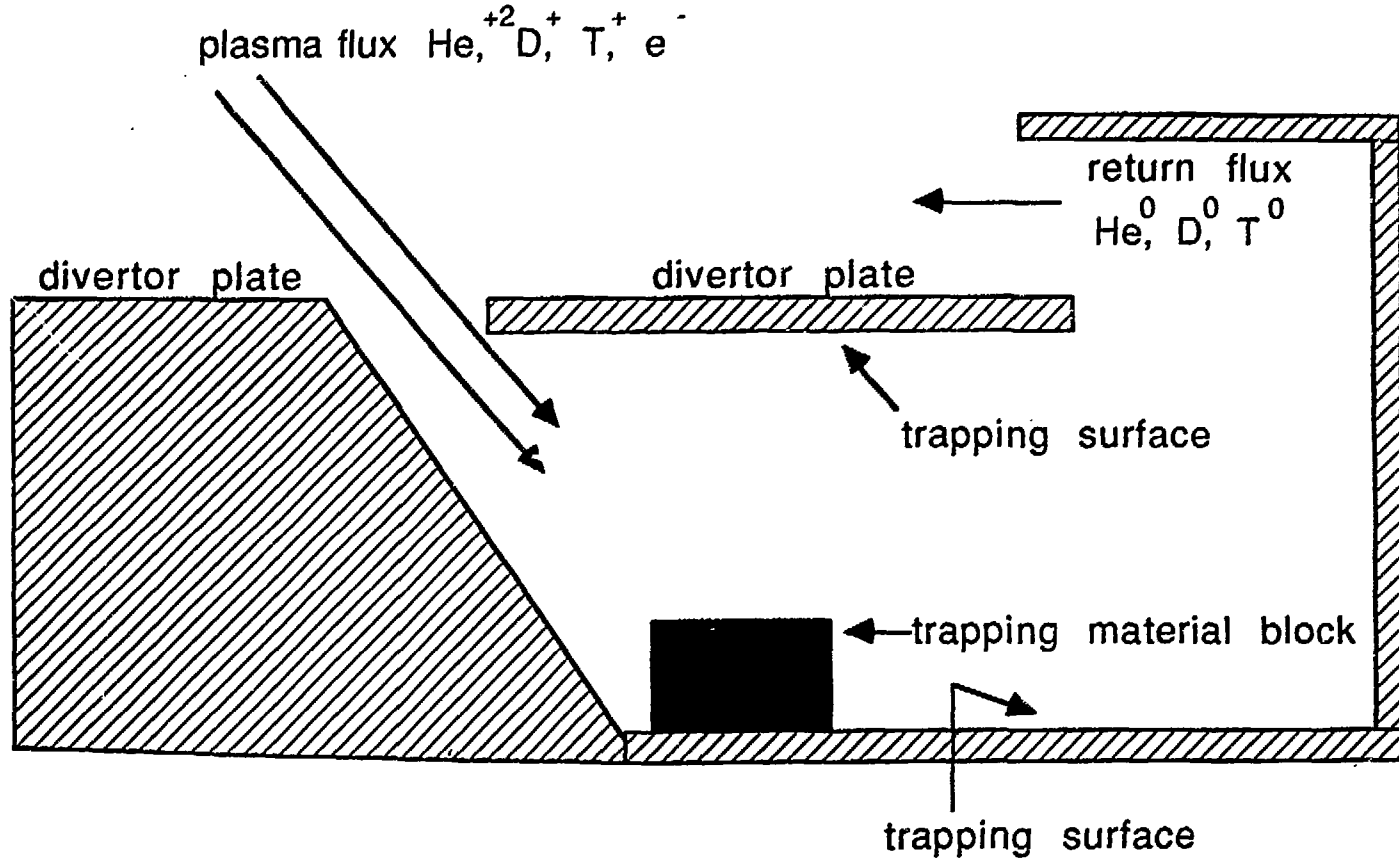
Parameter	Value
1. He trapping fraction	30 at%
2. Maximum temperature for trapping	$0.7 T_{\text{melt}}$
3. He sticking coefficient	0.25
4. Density of deposited material	$.8 \rho_0$
5. Thermal conductivity of deposited material	$.7 k_0$
6. Minimum energy for (substantial) trapping	30-50 eV

The slot divertor is shown schematically in Fig. 1. The system consists of a slot in the divertor plate and a box like (slot) region enclosure. Cooling manifolds and other structural elements are not shown but would typically be located at discrete toroidal locations. Some fraction of the hydrogen and helium flux to the divertor enters the slot region. The incoming flux impinges on a block of trapping material. Helium is reflected or desorbed from the block. Reflected helium impinges on the other slot surfaces at a substantial fraction of the initial energy. Fresh trapping material is continually deposited on these surfaces also. Some of the helium is trapped while the remaining helium and all of the hydrogen recycle back to the divertor zone through the opening near the end of the divertor plate. Trapping material introduced in the slot region would be unlikely to enter the divertor region plasma for two reasons: (1) there is only a small line-of-sight path to the plasma and (2) impurity ions entering the line-of-sight would tend to be strongly entrained in the incoming plasma and return to the trapping block.

An important consideration for the slot divertor is that a leading edge is created by the slot geometry. However, as will be shown, the heat load on the leading edge can be relatively modest.

In the concept shown, the trapping material is introduced simply by allowing the plasma to impinge on an uncooled block of trapping material. The block temperature will increase until the radiative loss equals the incoming heat flux. Calculations indicate that a surface temperature close to the

SELF-PUMPING SLOT DIVERTOR CONCEPT



6

Figure 1. Self-pumping slot divertor concept.

melting point would be reached. Evaporation from the block surface would serve to coat the slot surfaces. Alternatively, pellets, rods, etc. could be fed into the incoming plasma stream.

An initial design of a slot divertor has been developed and is summarized in Table 4. Heat and particle fluxes specified in Ref. 8 were used for design purposes. These are given for the outer separatrix region of the outer collector plate as:

$$q = q_0 e^{-x/\delta_E}$$

$$\Gamma_{DT} = \Gamma_0 e^{-x/\delta_p}$$

$$\Gamma_\alpha = .02 \Gamma_{DT}$$

where the fluxes are normal to the separatrix, $q_0 = 18 \text{ MW/m}^2$, $\Gamma_0 = 3 \times 10^{24} \text{ m}^{-2} \text{ s}^{-1}$, $\delta_E = 3 \text{ cm}$, $\delta_p = 9.4 \text{ cm}$, and x is the coordinate perpendicular to the separatrix.

If we design for a modest leading edge heat load of 1 MW/m^2 , the x coordinate at the leading edge is $x_0 = 8.67 \text{ cm}$. Allowing, somewhat arbitrarily, for a slot width of $\Delta x = 1 \text{ cm}$, or 4 cm along the divertor plate, the slot starts at $x_1 = 7.67 \text{ cm}$. The DT current to the slot is then:

$$I_{DT}^{\text{slot}} = 2\pi R_s \int_{x_1}^{x_0} \Gamma_{DT} dx$$

For the above values of x_0 , x_1 , and for $R_s = 5.5 \text{ m}$, $I_{DT}^{\text{slot}} = 4.4 \times 10^{23} \text{ s}^{-1}$. The helium current is:

TABLE 4. INTOR - Slot Self-Pumped Divertor

Parameter	Value
System	self-pumped helium removal using slot divertor
Trapping site	slot region
Location	near end of outer collector plate
Fusion power	570 MW
α -production rate	$2.0 \times 10^{20} \text{ s}^{-1}$
Trapping material evaporation rate	$6.7 \times 10^{20} \text{ s}^{-1}$
Trapping material	V (Ni, Fe)
Mass Utilization (for 75% D.F., 25% availability)	338 Kg/yr (vanadium)
Slot Width (perp.) to separatrix	1 cm
Slot width along divertor	4 cm
Heat flux on leading edge	1 MW/m ²
DT current to slot	$4.4 \times 10^{23} \text{ s}^{-1}$
He current to slot	$8.7 \times 10^{21} \text{ s}^{-1}$
Initial helium impact energy	~100 eV
Required helium trapping rate	$2 \times 10^{20} \text{ s}^{-1}$
Required local helium removal efficiency (helium removed/helium entering slot)	.023
Minimum required sticking coeff. (S)	.015
Predicted sticking coeff. (s)	.25
Estimated local removal eff. (S = .25)	.35
Lifetime	$\geq 2 \text{ yrs}$

$$I_{\alpha}^{\text{slot}} = .02 I_{DT} = 8.7 \times 10^{21} \text{ s}^{-1}$$

The required helium removal efficiency of the slot system is given by.

$$E = \frac{I_{\alpha}^0}{I_{\alpha}^{\text{slot}}}$$

where I_{α}^0 is the α -production rate. For $I_{\alpha}^0 = 2.0 \times 10^{20} \text{ s}^{-1}$, $E = .023$. In other words, the required removal efficiency is very modest; this is due to the very high particle fluxes in the high-recycling divertor regime.

The required efficiency could be reduced, if needed, by using an inboard slot system also, and/or by increasing the slot width.

The required rate of addition of trapping material is determined by the assumed saturation concentration of helium in the material and by the α -production rate. For a 30 at% concentration the required trapping material current is:

$$I_z^{\text{slot}} = \frac{I_{\alpha}^0}{.3} = 6.7 \times 10^{20} \text{ s}^{-1} .$$

The choice of trapping materials for this system is made easier by the fact that the heat load on the trapping sites is low, essentially negligible. A typical reference choice is vanadium, with nickel, iron, and the other materials mentioned above as alternatives.

The obtainable local helium removal efficiency (helium trapped/helium entering slot) can be roughly estimated as follows. The initial helium impingement energy is given by:

$$U_{\alpha}^0 = KT_e \left(1 + \frac{1}{2} \frac{M_{\alpha}}{M_{DT}} + 6 \right) \approx 8 KT_e$$

assuming $T_e = T_i$, a sheath potential of $3 KT_e$, a helium charge state of 2, and sound speed flow at the boundary. Therefore, for a plasma temperature of 10-15 eV, $U_{\alpha}^0 = 100$ eV. Typical particle and energy reflection coefficients of the trapping materials, at 100 eV, based on data for helium reflection from copper⁹ are $R_N = 0.5$, $R_E = 0.3$ for normal incidence and $R_N = 0.85$ and $R_E = .70$ for 60° from normal incidence. The average energy of the reflected helium is given by:

$$\bar{U}_{\alpha} = U_{\alpha}^0 \frac{R_E}{R_N} .$$

Based on calculations¹⁰ for glancing-angle magnetic field geometries, most helium would impinge at the contact-block at 60° or more from the normal. Reflected helium would therefore have an ~ 80 eV energy after one reflection and ~ 50 - 65 eV after two reflections (depending on the incident angular spectrum after one reflection). For a ~ 50 eV minimum effective trapping energy, helium can be trapped for two reflections and possibly for more. If the sticking coefficient is denoted by S , the probability of a helium atom being trapped in the slot region, assuming no trapping on the initial impingement and a 2 reflection maximum, is given by:

$$P = R_N S + R_N (1 - S) R_N S$$

Using $R_N = .85$ and $S = .25$ we have:

$$P = 0.35$$

which far exceeds the required value. Alternatively the minimum required value of sticking coefficient is determined by $P = E$ which yields $S^{\min} = .015$. This calculation ignores the effect of re-ionization of neutral helium by the incoming slot plasma which would tend to increase the trapping probability.

We conclude therefore, that only small values, i.e., 1-2% for sticking probabilities are required. The more critical issue therefore, is the trapping fraction.

The trapping material evaporation technique was assessed briefly as follows. A 2 year supply of vanadium requires (at 25% availability, 75% duty factor) 676 Kg or a block $2\pi \times 5.5$ m long, 4 cm wide and 8 cm high. For an uncooled block the surface temperature is given approximately by equating the incoming heat flux to the thermal radiation:

$$q \sin \theta = \epsilon \sigma T^4$$

where θ is the surface angle to the poloidal field lines, ϵ is the surface emissivity and σ is the Stephan-Boltzman constant. For $q = 1.0 \text{ MW/m}^2$, $\theta = 15^\circ$, $\epsilon = 0.4$; $T = 1821 \text{ K}$. This is about 85% of the melting point of vanadium. Evaporation varies exponentially with temperature. We therefore expect that adequate evaporation rates could be obtained by adjusting parameters, e.g., block geometry and plasma heat flux. In practice we would probably engineer for an over-supply of evaporated trapping material.

SYSTEM 2 - Divertor Plate Trapping

Mechanically, the simplest self-pumped system is to trap helium directly on the two divertor plates. In order to minimize the heat load on the trapping sites and to minimize plasma contamination, it may be most effective to trap on the outside portions of the plates. Impurity transport studies¹¹ have also shown that the helium flux may actually peak in this area. Characteristics of such a self-pumped system are shown in Table 5. Vanadium is a typical trapping material based on its estimated helium trapping properties, thermal properties, lack of deleterious activation, and because it is a medium Z material. Vanadium would be injected into the divertor plasma near the ends of the divertor plate at a vertical distance of up to several cm above the plate.

The main difference in impurity injection over hydrogen injection is the higher binding energy ($\sim 5 \text{ eV}$ vs. 0.005 eV). Also the shielding could be much better because of the $\sim Z^2$ dependence of impurity radiation in the appropriate

TABLE 5. INTOR - Self-Pumped Divertor, System #2

Parameter	Value
System	self-pumped helium removal using divertor plates
Trapping site	outer 15 cm of both divertor plates
Trapping site area	$\sim 10 \text{ m}^2$
Fusion power	570 MW
α -production rate	$2.0 \times 10^{20} \text{ s}^{-1}$
Trapping material injection rate	$6.7 \times 10^{20} \text{ s}^{-1}$
Trapping material	vanadium
Injection method	low speed pellets/dust
Injection Site	near first wall slightly (0-2 cm) above divertor plates
Energy of impinging helium	$\sim 100 \text{ eV}$
Mass utilization (for 75% D.F., 25% availability)	338 Kg/yr (vanadium)
Surface growth rate	$\sim 6 \text{ mm/yr}$ (vanadium)
Average surface heat load (transport + radiation + nuclear)	$< 1 \text{ MW/m}^2$
Helium removal efficiency (helium removed/helium crossing separatrix)	4.5%
Lifetime (for 75% D.F., 25% availability)	$> 2 \text{ yrs}$
Injected vanadium - steady-state concentration in main plasma	.01%

temperature range. To a first approximation, the lifetime would be longer by the ratio:

$$\frac{\tau_Z}{\tau_H} = \frac{5}{.005} \sim 1000 .$$

Thus, the pellets can go quite slowly or can be small, e.g., blown in like dust. We have made some calculations of impurity pellet ablation which indicate that the results are very model dependent. Qualitatively it appears that low velocity injection near the divertor edge is sufficient for ablation and subsequent transfer to the divertor plate. Control over where the pellets ablate could be achieved by choosing the appropriate pellet size.

The parameters of Table 5 are based on the material characteristics discussed earlier (Table 3). The injection rate of vanadium is based on the α -production rate and a 30 at% helium concentration in the trapping surface. The surface growth rate of 6 mm/yr is determined by the injection rate, trapping area, and trapping material density. The effective lifetime of the trapping portion of the divertor plate is determined by the heat flux, surface growth rate, and the maximum acceptable trapping material temperature. Based on these parameters, and extrapolating from the analysis of the first wall/limiter system of Ref. 3 we conclude that the lifetime of the INTOR self-pumped divertor plate should equal or exceed the 2 yr conventional divertor plate lifetime.

The helium pumping efficiency of this system was analyzed by Monte Carlo simulation using the ZTRANS Code.¹¹ The outer collector region for the high-recycling plasma regime was treated, we expect similar results for the inner collector region. An updated ion-thermal force term was used. Helium ions were launched along the separatrix as described in Ref. 11. Helium impinging on the outer 15 cm of the divertor plate was trapped with 25% probability, otherwise reflected as neutrals. No helium was pumped. The resulting helium removal efficiency of 4.5% is about eight times better than the predicted helium pumping efficiency of a pumped divertor with pumping at the outer collector plate only (and with the updated ion-thermal force term).

The other key issue for the divertor plate trapping system is plasma contamination by injected materials. To first order, vanadium etc. impinging on the divertor plate will sputter material via self-sputtering, but this material will be essentially 100% redeposited due to the very short ionization lengths for the high recycling plasma regime. The main contribution to plasma contamination then is impurity pellet ablation and transport above the divertor plate. The ZTRANS Code together with edge transport analysis were used to provide estimates of the contamination. For the ZTRANS simulations, tin ions ($Z=50$) were launched at various locations near the divertor plate, representing the introduction of ablated pellet material. The ions were launched with an initial charge state of unity. Tin ions were used as representing a rough average Z of the candidate trapping materials; the results however are fairly insensitive to the trapping material. The impurity particle was then followed by the code. A particle entering the plasma was re-launched along the separatrix. A particle history terminated upon hitting the divertor plate or first wall.

Table 6 summarizes the results of the simulations. As shown, the fraction of injected material entering the plasma depends on the launch location. In general, contamination can be minimized by keeping pellets confined to ~ 2 cm above the plate, or by confining pellets to the outside 15 cm and within ~ 5 cm above the plate. This seems reasonably attainable. It was also found that the trapping material flux to the plate correlates almost directly with the injection site, e.g., edge injection results in edge deposition on the plate.

The contamination fraction in the main plasma can be expressed as follows:

$$\frac{N_Z}{N_{DT}} = \frac{I_Z f_Z^P}{I_{DT}} \gamma$$

where I_Z is the injected current of trapping material in the scrapeoff zone, f_Z^P is the fraction (Table 6) of injected material entering the edge region, I_{DT} is the deuterium-tritium current entering (\sim leaving) the edge plasma, and γ is a parameter representing the effect of different confinement times of the impurities and the hydrogen in the plasma. A previous study¹² of impurity

transport in the edge and main plasma, using the WHIST 1-D plasma transport code found that a value of $\gamma \approx 0.25$ for non-neoclassical impurity transport applies for most impurity species. The large effect of impurity vs. hydrogen confinement times is attributed to the fact that the impurity source is at the plasma edge, whereas much of the fuel ion source is comprised of more deeply imbedded pellets (the remainder being supplied by recycling, which is also a source in the context of this discussion). Thus, a newly introduced impurity atom in the edge plasma has a greater chance of being promptly lost than the average fuel atom and, as confirmed by the code output, the impurity confinement times are commensurately shorter. Using a typical value of $f_Z^P = .025$, and for $\gamma = .25$, $I_Z = 7 \times 10^{20} \text{ s}^{-1}$, and $I_{DT} = 4 \times 10^{22} \text{ s}^{-1}$, the contamination fraction is then estimated at $\frac{N_Z}{N_{DT}} = 1 \times 10^{-4}$. This would be an acceptable concentration for a high Z material and is acceptable by a factor of 10 for vanadium. Although calculations of this nature, are of necessity speculative, because of the unverified nature of impurity transport coefficients, one concludes that there is a reasonable chance of achieving acceptably low central plasma impurity concentrations of the trapping material.

TABLE 6.

Fraction of Injected Trapping Material Entering the Edge Plasma as a Function of Injection Location. From XTRANS Monte Carlo Simulations for S_N Injection.

Injection Site	f_Z^P , Fraction Entering Plasma
uniform along plate, 2 cm above plate	.008
middle 5 cm of plate, 3 cm above plate	.08
outer 15 cm of plate, 3 cm above plate	.01
outer 15 cm of plate, 5 cm above plate	.03
outer 15 cm of plate, 10 cm above plate	.05

Conclusion

Based on the present analysis, self-pumping impurity control appears to be both feasible and advantageous for INTOR. The slot divertor offers the possibility of a simple, passive, helium removal system. Plate trapping is even simpler mechanically but involves more uncertain impurity transport properties.

As discussed, the material properties assumed in this study are based on a limited experimental data base. Several important factors need be studied experimentally to firmly establish the parameters for helium retention. In particular, experiments with codeposition of trapping material, hydrogen, and helium, at representative energies are required.

Future design efforts in this area would include a structural design of the slot divertor and a further characterization of the slot region plasma.

References

1. J. N. Brooks and R. F. Mattas, J. Nucl. Mat. 121(1984) 392.
2. A. E. Pontau, W. Bauer, and R. W. Conn, J. Nucl. Mat. 93&94(1980) 564.
3. C. C. Baker et al., "Tokamak Power Systems Studies," Argonne National Laboratory, ANL/FPP/85-2 (19).
4. D. J. Reed et al., Vacuum 24, No. 4 (1974) 179.
5. P. Bailey et al., Rad. Effects, 78 (1983) 133.
6. R. Kelly and C. Jech, J. Nucl. Mater. 30, (1969) 122.
7. W. D. Wilson and C. L. Bisson, Rad. Effects Vol. 22 (1974) 1.
8. INTOR - Phase Two A, Part II, IAEA STI/PUB/714, Vienna (1986) p. 127.
9. O. S. Oen and M. T. Robinson, Nucl. Instr. Meth., 132 (1976) 647.
10. R. Chodura, Phys. Fluids 25(9) (1982) 1628.
11. J. N. Brooks, "Two Dimensional Impurity Transport Calculations for a High Recycling Divertor," Seventh International Conf. on Plasma-Surface Interactions in Controlled Fusion Devices, J. Nuc. Mat. (to be published).
12. W. K. Terry, J. N. Brooks, and C. D. Boley, Fus. Tech. 7(1985) 158.

DISTRIBUTION LIST FOR ANL/FPP/TM-212

Internal:

C. Baker	D. Gruen	C. Reed
M. Billone	A. Hassanein	D. Smith
J. Brooks (10)	T. Hua	H. Stevens
Y. Cha	C. Johnson	D. Sze
O. Chopra	A. Krauss	L. Turner
R. Clemmer	Y. Liu	T. Yule
D. Ehst	B. Loomis	FPP Files (11)
K. Evans	S. Majumdar	ANL Contract File
P. Finn	R. Mattas	ANL Libraries
Y. Gohar	B. Picologlou	ANL Patent Dept.
L. Greenwood	K. Porges	TIS Files (5)

U.S. Department of Energy:

External:

UC-20 Distribution (103)
Manager, Chicago Operations Office, DOE
M. Cohen, Office of Fusion Energy, DOE
G. Haas, Office of Fusion Energy, DJE
P. Stone, Office of Fusion Energy, DOE
M. Abdou, University of California, Los Angeles
W. Bauer, Sandia Laboratories
D. Cohn, Massachusetts Institute of Technology
R. Conn, University of California, Los Angeles
J. Davis, McDonnell Douglas Astronautics Company
S. Dean, Fusion Power Associates
K. Dippel, KFA, Julich, FRG
T. Drolet, Ontario Hydro, CANADA
H. Furth, Princeton Plasma Physics Laboratory
W. Gauster, Sandia National Laboratory, Albuquerque
P. Gierszewski, Canadian Fusion Fuels Technology Project
C. Henning, Lawrence Livermore National Laboratory
R. Krakowski, Los Alamos National Laboratory
G. Kulcinski, University of Wisconsin, Madison
G. Logan, Lawrence Livermore National Laboratory
R. McGrath, Sandia National Laboratory, Albuquerque
G. Miley, University of Illinois-Urbana
D. Post, Princeton Plasma Physics Laboratory
P. Rutherford, Princeton University
J. Schmidt, Princeton Plasma Physics Laboratory
T. Shannon, Fusion Engineering Design Center/Oak Ridge National Laboratory
W. Stacey, Jr., Georgia Institute of Technology
D. Steiner, Rensselaer Polytechnic Institute
A. Tobin, Grumman Aerospace Corporation
T. Tomabechi, Japan Atomic Energy Research Institute, JAPAN
W. Verbeeck, CEC, BELGIUM

Prof. Vetter, Kernforschungszentrum Karlsruhe und Verwaltung, GERMANY
Bibliothek, Max-Planck-Institute für Plasmaphysik, WEST GERMANY
C.E.A. Library, Fontenay-aux-Roses, FRANCE
Librarian, Culham Laboratory, ENGLAND
Library Laboratorio Gas Ionizzati, ITALY
Thermonuclear Library, Japan Atomic Energy Research Institute, JAPAN